ChemComm

COMMUNICATION

View Article Online
View Journal | View Issue

Check for updates

Cite this: *Chem. Commun.*, 2025, **61**, 1200

Received 1st October 2024,
Accepted 3rd December 2024

DOI: 10.1039/d4cc05188b

rsc.li/chemcomm

Open Access Article. Published on 04 Disember 2024. Downloaded on 12/05/2026 10:48:53 PTG.
This article is licensed under a Creative Commons Attribution-NonCommercial 3.0 Unported Licence.

Expression of hyperconjugative stereoelectronic interactions in borazines†

Vivek Chandrakant Wakchaure, [a] Jacopo Dosso, [b] Martina Crosta, [a] Hanspeter Kählig,[a] Benjamin D. Ward [b] and Davide Bonifazi *[a]

This paper discusses hyperconjugative stereoelectronic effects in borazines. A series of alkyl-substituted borazines were synthesized and analysed by NMR spectroscopy and X-ray diffraction. Supported by NBO analyses, the significant decreases in $^1J_{CH}$ coupling constant for the CH groups adjacent to the boron atoms are consistent with the presence of $\sigma_{C-H} \rightarrow \pi^*_{B=N}$ and $\sigma_{C-H} \rightarrow \sigma^*_{B-N}$ interactions. These interactions lower the electrophilicity of boron atoms, enhancing moisture stability and establishing these molecules as valuable scaffolds in synthetic chemistry and materials science.

The significance of BN-doped molecular scaffolds has recently surged due to their broad applications in optoelectronic devices,[1–4] thermal management materials,[5] and catalysis.[6] Among these, hexasubstituted borazine is an attractive option for BN-based architectures.[7] The borazine core's susceptibility to hydrolysis in water has hindered its widespread use.[8] To prevent borazine hydrolytic decomposition, bulky aryl groups can be added to the boron atom, where *ortho*-substituents create steric hindrance shielding B-atoms from water.[9] In another architecture, amino groups were used to stabilize the borazine ring within a hybrid cyclomatrix polymer.[9f] In search of other approaches preventing hydrolysis, we noticed that *B*,*B*′,*B*″-trialkyl-*N*,*N*′,*N*″-triphenyl borazines (alkyl moieties being i- and *n*-propyl, i- and *n*-butyl) exhibit remarkable counterintuitive moisture resistance when compared to its aryl-substituted congeners.[10] A comprehensive understanding of the factors affecting the stability of these molecules is still lacking. It is possible that hyperconjugative stereoelectronic interactions occur between the electron-donating alkyl groups and the electrophilic borazine ring (Fig. 1b),[11] similar to what is seen in trialkyl boranes.[9h,i] With this hypothesis in mind, in this paper, we address the presence of such hyperconjugative effects through NMR spectroscopy and X-ray investigations of a series of *B*-alkyl borazine derivatives.[12] Theoretical modeling further supported these studies by elucidating the molecular orbitals involved in those interactions.[13] Three types of alkyl groups to be attached to the boron centres were chosen: $-CH_3$, $-CH_2-$, and –CH–. While molecules **1a–b** bear methyl substituents, **2a–e** and **3a–b** feature methylene (as $-^n$Bu, $-^n$Hex, $-^n$Oct, benzyl and (trimethylsilyl)methyl substituents) and methine (as $-^i$Pr and cyclohexyl substituents) substitutions on the boron atoms (Fig. 1a), respectively.

The synthesis for these alkyl borazines have been carried out by adapting known protocols.[9c] Intermediate trichloroborazole (**BNCl**) was prepared by refluxing aniline with BCl_3 in toluene (Scheme S1, ESI†). The reaction of **BNCl** with the respective organoalkyl-lithium/Grignard nucleophiles in THF gave the final product in good yields (61–74%, Fig. 1a and Scheme S2, ESI†). The structures of all alkyl borazines were characterized by ^{1}H and ^{13}C NMR spectroscopy, and with high-resolution mass spectrometry (Fig. S1–S48, ESI†) and selected structures by single-crystal X-ray diffraction analysis. All *B*,*B*′,*B*″-trialkyl borazine derivatives exhibited low reactivity towards moisture, allowing them to be handled in the air without precautions and purified through column chromatography. Thermogravimetric analysis (TGA) indicated that all derivatives remain stable above 200 °C (Fig. S49–S51, ESI†).

X-ray diffraction investigations of selected borazine derivatives were first attempted to shed further light on their structural properties (Fig. 2a–f and Tables S1–S6 and Fig. S52–S57,

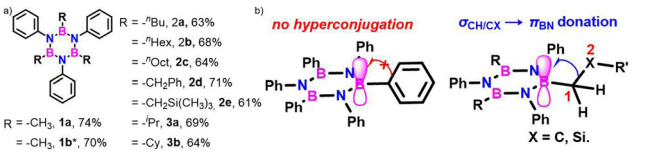

Fig. 1 (a) Alkyl borazines studied in this work (*2′,6′-dimethyl-[1,1′-biphenyl]-4-amine used for the synthesis). (b) Stereoelectronic interactions in *B*-aryl and *B*-alkyl borazines.

[a] *Institute of Organic Chemistry, Faculty of Chemistry, University of Vienna, Währinger Strasse 38, 1090, Vienna, Austria. E-mail: davide.bonifazi@univie.ac.at*
[b] *School of Chemistry, Cardiff University, Main Building, Park Place, Cardiff CF10 3AT, UK*

† Electronic supplementary information (ESI) available. CCDC 2261150, 2261151, 2280127, 2280128, 2284380 and 2307378. For ESI and crystallographic data in CIF or other electronic format see DOI: https://doi.org/10.1039/d4cc05188b

This journal is © The Royal Society of Chemistry 2025

Open Access Article. Published on 04 Disember 2024. Downloaded on 12/05/2026 10:48:53 PTG.
This article is licensed under a Creative Commons Attribution-NonCommercial 3.0 Unported Licence.

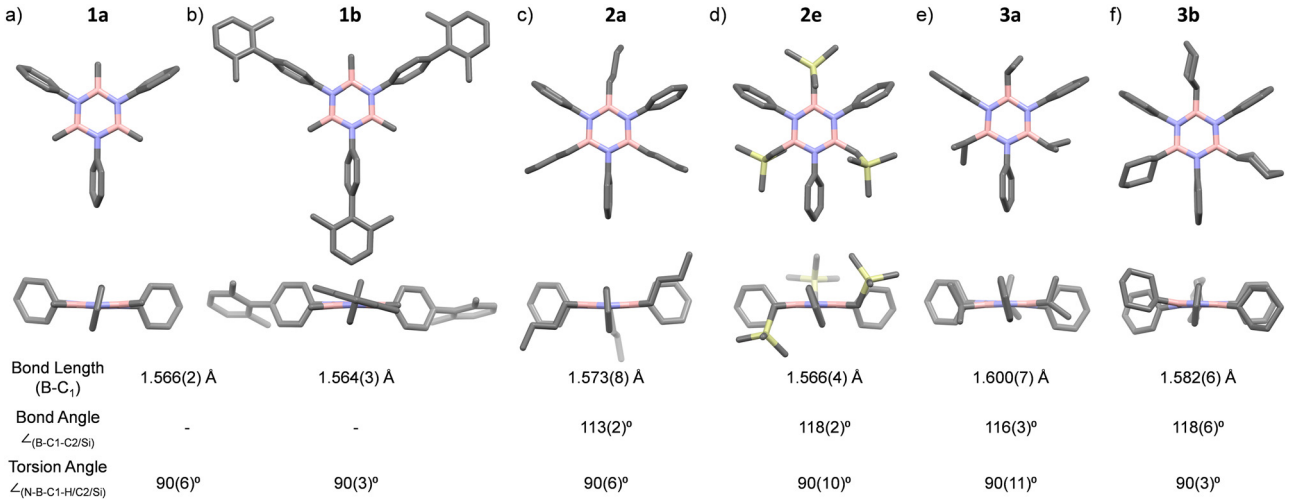

Fig. 2 Single-crystal X-ray structures of borazines and relevant structural parameters (a) **1a**, *C*2/*c*, (b) **1b**, *C*2/*c*, (c) **2a**, *Cc*, (d) **2e**, $P2_1/c$, (e) **3a**, $P\bar{1}$, and (f) **3b**, $Pna2_1$. Grey: C, pink: B, yellow: Si, and blue: N. The torsion angles are the average of the values measured for C–H/C/Si bonds that display an orientation that is close to that of perpendicularity.

ESI†). In all derivatives, the central borazine ring displays a nearly flat geometry, with average $\angle_{N-B-N}$ and $\angle_{(B-N-B)}$ angles of 116.2(4)° and 123.7(4)°, respectively, and with typical B–C_1 bond lengths of 1.575(14) Å (Fig. 2).[11c] For molecules **2a**, **3a**, and **3b**, the C_1–C_2 bond lengths (average value ∼1.526(4) Å) fall within the expected range for corresponding single bonds.[11a] The average torsional angles $\angle_{(N-B-C1-H/C2/Si)}$, describing the relative orientation of the B–C–H/C/Si bonds to the borazine ring, are ∼90° for all borazines (Fig. 2). This perpendicular arrangement of the C–H/C/Si bonds is to be expected when in the presence of a hyperconjugation. Moreover, the bond angle $\angle_{(B-C1-C2)}$ for **2a**, **3a** and **3b** is found to be 113(2)°, 116(3)° and 118(6)°, respectively. Similarly, the bond angle $\angle_{(B-C1-Si)}$ is 118(2)° for molecule **2e** (Fig. 2). These $\angle_{(B-C1-H/C2/Si)}$ angles are wider than those between C(sp^3), again suggesting that a hyperconjugative interaction is at play.[11a]

Considering that one-bond NMR spin–spin coupling constants are experimental probes for determining any stereo-electronic interactions (Perlin effect),[14] we tackled the determination of the ^1H–^{13}C coupling constants (J_{CH}) of the C–H bonds connected to the B-atoms by analysis of either the carbon satellite signals in the ^1H NMR spectra or the doublet cross peaks in proton-coupled Heteronuclear single quantum coherence (HSQC) experiments (Fig. 3). For **1a** and **1b**, the experimental $^1J_{CH}$ value for the B–Me groups is 116.4 and 116.6 Hz (Fig. 3a), respectively, which is lower than that of the Me group

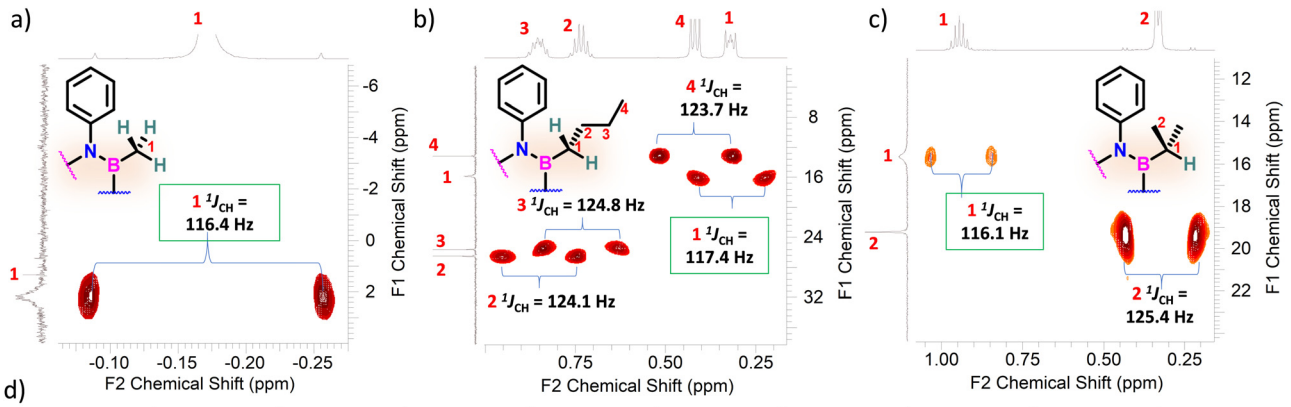

d)

Molecule	1a	1b	2a	2b	2c	2d	2e	3a	3b
$1\,^1J_{CH}$ in Hz	116.4	116.6	117.4	117.3	117.0	117.8	112.7	116.1	112.3
$2\,^1J_{CH}$ in Hz	-	126.6	124.1	125.5	125.8	-	118.4	125.4	126.0
$1\,^1J_{CSi}$ in Hz	-	-	-	-	-	-	38.6	-	-
$2\,^1J_{CSi}$ in Hz	-	-	-	-	-	-	50.9	-	-

Fig. 3 Excerpts of the HSQC spectra displaying the relevant $^1J_{CH}$ coupling constants for (a) **1a**, (b) **2a**, and (c) **3a** and. (d) $1\,^1J_{CH}$, $2\,^1J_{CH}$, $1\,^1J_{CSi}$ and $2\,^1J_{CSi}$ values for each alkyl borazines.

Open Access Article. Published on 04 Disember 2024. Downloaded on 12/05/2026 10:48:53 PTG.
This article is licensed under a Creative Commons Attribution-NonCommercial 3.0 Unported Licence.

in the same molecule ($^2J_{CH}$ = 126.6 Hz, Fig. S8 and S13, ESI†). Similarly, the $^1J_{CH}$ values for molecules **2a–e** are within the 112 Hz to 118 Hz range, which is also lower than the other J_{CH} values (Fig. 3b and Fig. S18, S23, S28, S33 and S38, ESI†). Further, by examining the ^{29}Si NMR spectrum of molecule **2e**, we could determine the coupling constants $^1J_{CSi}$ for –CH_2– and –CH_3 groups attached to the Si-atom. The results indicate that $^1J_{CSi}$ of –CH_2– exhibits a value of ∼12.3 Hz lower than that measured with –CH_3 (Fig. S38, ESI†). This suggests that the C–Si bond experiences an elongation that one could attribute to a hyperconjugation. For **3a** and **3b**, the $^1J_{CH}$ values are 116.1 and 112.3 Hz, respectively (Fig. 3c and Fig. S43 and S48, ESI†). Notably, these couplings were the lowest among the series. These observations are in line with the X-ray-measured $\angle_{(B\text{–}C1\text{–}C2)}$ angle values (Fig. 2), confirming strong hyperconjugative interactions between the B(p_z) orbital and the $\sigma_{C\text{–}H}$, $\sigma_{C\text{–}C}$ and $\sigma_{C\text{–}Si}$ bonds of the relevant substituents.

DFT calculations were employed to explore hyperconjugation, with bonding analysed *via* natural bonding orbital (NBO) analyses.[13c] The findings revealed weak interactions between the $\sigma_{C\text{–}H}$ and $\sigma_{C\text{–}C}$ orbitals and both the $\pi^*_{B=N}$ and $\sigma^*_{B\text{–}N}$ orbitals for all derivatives. The $\sigma_{C\text{–}H}$ orbital, positioned perpendicularly to the ring, exhibited significant overlap with the π* orbital. For **1a** and **1b**, the optimised structure contains a C–H lying orthogonal to the borazine plane (Fig. 2a and b) and two that are at the midpoint between the orthogonal and parallel planes ($\sigma_{C\text{–}H} \rightarrow \pi^*_{B=N}$ and $\sigma_{C\text{–}H} \rightarrow \sigma^*_{B\text{–}N}$ in Fig. 4a and Fig. S58, ESI†). Since the overlap between $\sigma_{C\text{–}H}$ and the given unoccupied orbitals depends on the orientation of the substituent, the stabilisation energy (E_2) associated with these interactions was computationally probed as a function of the angle between the proximal $\sigma_{C\text{–}H/C/Si}$ orbital and the borazine ring upon rotation about the B–C bond (molecule **1a** in Fig. 4). As expected, the $\sigma_{C\text{–}H} \rightarrow \pi^*_{B\text{–}N}$ interaction is the strongest, 6.5 kcal mol^{-1}, when the C–H bond lies perpendicular to the BN ring as this orientation gives the most significant orbital overlap between the $\sigma_{C\text{–}H}$ and $\pi^*_{B=N}$ orbitals. As the Me group is rotated, E_2 decreases, and no interaction is detected with $\angle_{(N\text{–}B\text{–}C1\text{–}H)}$ values <20°. Conversely, the $\sigma_{C\text{–}H} \rightarrow \sigma^*_{B\text{–}N}$ interaction gives the strongest stabilisation, 3.51 kcal mol^{-1}, when the C–H bond lies in the same plane as the BN ring. The effect is not as pronounced as the $\sigma_{C\text{–}H} \rightarrow \pi^*_{B\text{–}N}$, but it contributes conferring an additional stabilisation. Similarly, NBO analysis shows both $\sigma_{C\text{–}H} \rightarrow \pi^*_{B=N}$ and $\sigma_{C\text{–}H} \rightarrow \sigma^*_{B\text{–}N}$ interactions in the case of –CH_2– and –CH– (**3a–b**) substitutions (Fig. S59–S67, ESI†). Also, the stabilisation energies were probed for proximal $\sigma_{C\text{–}C/Si}$ bonds (Fig. S61, ESI†).

Interactions between the $\sigma_{C\text{–}C}$ and BN ring orbitals are significant when sterically demanding alkyl groups prevent the C–H group from lying perpendicular to the ring, and $\sigma_{C\text{–}C} \rightarrow \sigma^*_{B\text{–}N}$ interactions are present in **2a–e** and **3a–b** (Fig. S60–S66, ESI†) but offered less of a stabilising effect than those involving $\sigma_{C\text{–}H}$ (Fig. 4b). Notably, $\sigma_{C\text{–}Si} \rightarrow \pi^*_{B=N}$ and $\sigma_{C\text{–}Si} \rightarrow \sigma^*_{B\text{–}N}$ interactions in **2e** displayed stronger stabilization than those with $\sigma_{C\text{–}C}$ (Fig. S61, ESI†). The maximum E_2 value is observed at the torsion angles $\angle_{(N\text{–}B\text{–}C1\text{–}H/C2/Si)}$ of ∼90° and 0° for $\sigma_{CH/CC/CSi} \rightarrow \pi^*_{B=N}$ and $\sigma_{CH/CC/CSi} \rightarrow \sigma^*_{B\text{–}N}$ interactions, respectively (Table 1). We evaluate energy changes for **1a** using a different basis set and calculation function (Fig. S67, ESI†), confirming the reliability of the data.

Further, we calculated the NMR coupling constant using the GIAO method.[15] The results (Table S7, ESI†) show that the difference ΔJ between $^1J_{C1H}$ and $^1J_{C2H}$ is 6 to 10 Hz, which is in agreement with the experimental values. Similarly, the calculated ΔJ between $^1J_{C1Si}$ and $^1J_{C2Si}$ in **2e** is 12 Hz, matching the experimental data (Table S8, ESI†). We examined the isodesmic reactions with borazine **3**, which has Me and Ph moieties on the N and B atoms (ESI,† Section S7.2.3). Our findings revealed higher values for enthalpy (+18.5 kcal mol^{-1}) and Gibbs free energy (+17.4 kcal mol^{-1}) compared to congener **1a**, highlighting the significant impact of hyperconjugation. NBO interactions in Me- and Et-substituted benzene congeners ($\mathbf{4_{Me}}$ and $\mathbf{4_{Et}}$) yielded $\sigma_{C\text{–}H} \rightarrow \pi^*_{C=C}$ values of 5.1 and 3.4 kcal mol^{-1}. These values indicate that $\mathbf{4_{Me}}$ and $\mathbf{4_{Et}}$ exhibit reduced hyperconjugation than their BN counterparts, as evidenced by their higher $^1J_{C1H}$ and $^1J_{C2H}$ values than those of **1a** and **2b**, Table S9, ESI†).

As a proof of concept exploiting the hyperconjugation to stabilize borazine derivatives, we successfully prepared crosslinked borazine-based polymers[9f] using either 1,6-dilithium hexane or 1,8-dilithium octane as nucleophiles (Fig. 5a). The insoluble nature of the obtained materials in common organic solvents suggests the presence of a crosslinked structure. Also, it exhibits hydrolytic stability. Solid-state ^{13}C NMR spectra

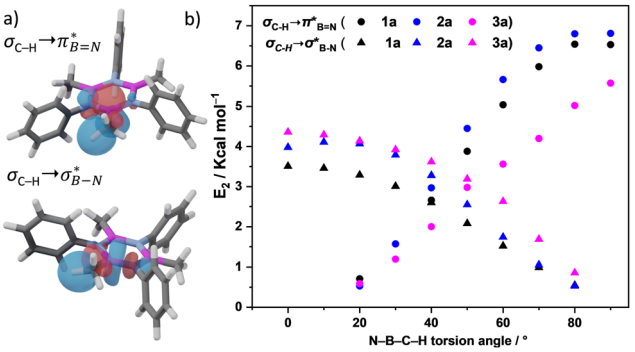

Fig. 4 (a) NBO for $\sigma_{C\text{–}H} \rightarrow \pi^*_{B=N}$ and $\sigma_{C\text{–}H} \rightarrow \sigma^*_{B\text{–}N}$ **1a** (PBE/def2-TZVP, orbitals with only one B-atom are shown), (b) hyperconjugative energies upon rotation of the *B*-alkyl group.

Table 1 Stabilisation energies (E_2) as a function of the torsional angle (90° for $\sigma_{CH/CC/CSi} \rightarrow \pi^*_{B=N}$ and 0° for $\sigma_{CH/CC/CSi} \rightarrow \sigma^*_{B\text{–}N}$ (PBE/def2-TZVP)

	E_2/kcal mol^{-1}								
Molecule	**1a**	**1b**	**2a**	**2b**	**2c**	**2d**	**2e**	**3a**	**3b**
$\sigma_{C\text{–}H} \rightarrow \pi^*_{B=N}$	6.53	6.48	6.81	6.40	6.40	5.70	5.28	5.57	4.70
$\sigma_{C\text{–}H} \rightarrow \sigma^*_{B\text{–}N}$	3.51	3.52	3.98	3.99	3.99	3.96	4.37	4.36	4.39
$\sigma_{C\text{–}C} \rightarrow \pi^*_{B=N}$	—	—	3.83	3.87	3.80	2.66	—	3.85	3.47
$\sigma_{C\text{–}C} \rightarrow \sigma^*_{B\text{–}N}$	—	—	1.28	1.28	1.28	1.04	—	1.52	1.41
$\sigma_{C\text{–}Si} \rightarrow \pi^*_{B=N}$	—	—	—	—	—	—	7.94	—	—
$\sigma_{C\text{–}Si} \rightarrow \sigma^*_{B\text{–}N}$	—	—	—	—	—	—	2.22	—	—

This journal is © The Royal Society of Chemistry 2025

Open Access Article. Published on 04 Disember 2024. Downloaded on 12/05/2026 10:48:53 PTG.
This article is licensed under a Creative Commons Attribution-NonCommercial 3.0 Unported Licence.

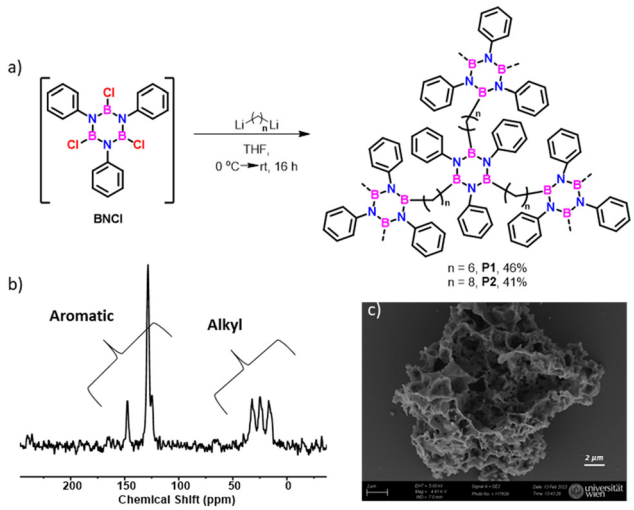

Fig. 5 (a) Synthesis of cross-linked polymers **P1** and **P2**, (b) solid-state $^{1}H \rightarrow {}^{13}C$ cross-polarization and magic angle spinning (CPMAS) NMR spectrum of **P1**, and (c) SEM images of **P1** (see CPMAS NMR spectrum for reference borazine **2a** in Fig. S68, ESI†).

(Fig. 5b and Fig. S68–S70, ESI†) distinctly displayed aromatic and aliphatic signals corresponding to the phenyl ring and alkyl chain on the borazine structure. Scanning electron microscope (SEM) analyses revealed the morphology of **P1** and **P2** polymers, showing aggregates and macroscopic porosity (Fig. 5c and Fig. S71 and S72, ESI†). TGA analysis indicated approximately 50% weight loss (up to 500 °C), which matches the alkyl moieties' loss (Fig. S73, ESI†).

In conclusion, our studies into alkyl borazines using NMR spectroscopy have revealed key insights into stereoelectronic interactions. The findings confirm the existence of interactions between the C_1–H, C_1–C_2, and C_1–Si bonds of the *B*-alkyl group with the $\pi^*_{B=N}$ orbital of the BN ring. Computational analyses provide a nuanced understanding of the interplay between the $\sigma_{C-H/C/Si}$ orbitals and both the $\pi^*_{B=N}$ and σ^*_{B-N} orbitals. As proof of principle, we have developed stable crosslinked borazine polymers that demonstrate moisture resistance. Our findings enhance the knowledge of borazines and expand their applications, offering exciting opportunities for using inorganic benzene in new materials and advanced chemistry.

D. B. acknowledges the EU (MSCA-ITN-ETN, STiBNite, no. 956923 & HORIZON-IA, DecoChrom, no. 760973) and the University of Vienna for funding; we acknowledge access to the HPC service (ARCCA) at Cardiff University, we thank Dr D. Romito (Vienna) and Dr P. K. Mondal (Elettra Trieste) for help in some X-ray analyses.

Data availability

The data supporting this article are in the ESI,† while the original data are available from the authors upon request.

Conflicts of interest

There are no conflicts to declare.

Notes and references

1 (*a*) I. H. T. Sham, C. C. Kwok, C. M. Che and N. Zhu, *Chem. Commun.*, 2005, 3547–3549; (*b*) D. Bonifazi, F. Fasano, M. M. Lorenzo-Garcia, D. Marinelli, H. Oubaha and J. Tasseroul, *Chem. Commun.*, 2015, **51**, 15222–15236; (*c*) D. Marchionni, S. Basak, A. N. Khodadadi, A. Marrocchi and L. Vaccaro, *Adv. Funct. Mater.*, 2023, **33**, 2303635; (*d*) I. Neogi and A. M. Szpilman, *Synthesis*, 2022, 1877–1907.
2 (*a*) Z. Huang, S. Wang, R. D. Dewhurst, N. V. Ignat'ev, M. Finze and H. Braunschweig, *Angew. Chem., Int. Ed.*, 2020, **59**, 8800–8816; (*b*) S. Madayanad Suresh, D. Hall, D. Beljonne, Y. Olivier and E. Zysman-Colman, *Adv. Funct. Mater.*, 2020, **30**, 1908677.
3 (*a*) J. Dosso, J. Tasseroul, F. Fasano, D. Marinelli, N. Biot, A. Fermi and D. Bonifazi, *Angew. Chem., Int. Ed.*, 2017, **56**, 4483–4487; (*b*) S. Oda and T. Hatakeyama, *Bull. Chem. Soc. Jpn.*, 2021, **94**, 950–960; (*c*) J. Kashida, Y. Shoji, Y. Ikabata, H. Taka, H. Sakai, T. Hasobe, H. Nakai and T. Fukushima, *Angew. Chem., Int. Ed.*, 2021, **60**, 23812–23818.
4 (*a*) S. Wang, *Coord. Chem. Rev.*, 2001, **215**, 79–98; (*b*) Y.-L. Rao and S. Wang, *Inorg. Chem.*, 2011, **50**, 12263–12274.
5 (*a*) M. R. H. Mazumder, L. D. Mathews, S. Mateti, N. V. Salim, J. Parameswaranpillai, P. Govindaraj and N. Hameed, *Appl. Mater. Today*, 2022, **29**, 101672; (*b*) Y. Luo, L. Zou, J. Qiao, J. Zhang, K. Liu, H. Wu, P. Lin and Y. Chen, *ACS Appl. Energy Mater.*, 2022, **5**, 11591–11603.
6 A. K. Thakur, K. Kurtyka, M. Majumder, X. Yang, H. Q. Ta, A. Bachmatiuk, L. Liu, B. Trzebicka and M. H. Rummeli, *Adv. Mater. Interfaces*, 2022, **9**, 2101964.
7 (*a*) A. Wakamiya, T. Ide and S. Yamaguchi, *J. Am. Chem. Soc.*, 2005, **127**, 14859–14866; (*b*) S. Kervyn, N. Kalashnyk, M. Riello, B. Moreton, J. Tasseroul, J. Wouters, T. S. Jones, A. De Vita, G. Costantini and D. Bonifazi, *Angew. Chem., Int. Ed.*, 2013, **52**, 7410–7414; (*c*) J. Dosso, T. Battisti, B. D. Ward, N. Demitri, C. Hughes, A. P. Williams, K. D. M. Harris and D. Bonifazi, *Chem. – Eur. J.*, 2020, **26**, 6608–6621.
8 T. Yoshizaki, H. Watanabe and T. Nakagawa, *Inorg. Chem.*, 1968, **7**, 422–429.
9 (*a*) K. Nagasawa, *Inorg. Chem.*, 1966, **5**, 442–445; (*b*) S. Kervyn, O. Fenwick, F. Di Stasio, Y. S. Shin, J. Wouters, G. Accorsi, S. Osella, D. Beljonne, F. Cacialli and D. Bonifazi, *Chem. – Eur. J.*, 2013, **19**, 7771–7779; (*c*) D. Marinelli, F. Fasano, B. Najjari, N. Demitri and D. Bonifazi, *J. Am. Chem. Soc.*, 2017, **139**, 5503–5519; (*d*) N. Kalashnyk, P. Ganesh Nagaswaran, S. Kervyn, M. Riello, B. Moreton, T. S. Jones, A. De Vita, D. Bonifazi and G. Costantini, *Chem. – Eur. J.*, 2014, **20**, 11856–11862; (*e*) J. Dosso, D. Marinelli, N. Demitri and D. Bonifazi, *ACS Omega*, 2019, **4**, 9343–9351; (*f*) N. A. Riensch, A. Deniz, S. Kühl, L. Müller, A. Adams, A. Pich and H. Helten, *Polym. Chem.*, 2017, **8**, 5264; (*g*) J. R. Sanzone, C. T. Hu and K. A. Woerpel, *J. Am. Chem. Soc.*, 2017, **139**, 8404–8407; (*h*) A. R. Cowley, A. J. Downs, S. Marchant, V. A. Macrae, R. A. Taylor and S. Parsons, *Organometallics*, 2005, **24**, 5702–5709; (*i*) B. Wrackmeyer and O. L. Tok, *Z. Naturforsch. B*, 2005, **60**, 259–264.
10 (*a*) S. J. Groszos and S. F. Stafiej, *J. Am. Chem. Soc.*, 1958, **80**, 1357–1360; (*b*) J. H. Smalley and S. F. Stafiej, *J. Am. Chem. Soc.*, 1959, **81**, 582–586; (*c*) R. J. Brotherton and A. L. McCloskey, *Adv. Chem.*, 1964, **42**, 131–138; (*d*) I. B. Atkinson, D. C. Blundell and D. B. Clapp, *J. Inorg. Nucl. Chem.*, 1972, **34**, 3037–3041.
11 (*a*) A. H. Maulitz, P. Stellberg and R. Boese, *J. Mol. Struct.: THEOCHEM*, 1995, **338**, 331–340; (*b*) I. V. Alabugin, *Stereoelectronic Effects: A Bridge Between Structure and Reactivity*, Wiley, Hoboken, 2016; (*c*) R. Boese, A. H. Maulitz and P. Stellberg, *Chem. Ber.*, 1994, **127**, 1887–1889.
12 (*a*) G. Cuevas and E. Juaristi, *J. Am. Chem. Soc.*, 2002, **124**, 13088–13096; (*b*) R. Boese, D. Blaser, N. Niederprum, M. Nusse, W. A. Brett, P. V. R. Schleyer, M. Buhl and N. J. R. V. E. Hommes, *Angew. Chem., Int. Ed. Engl.*, 1992, **31**, 314–316.
13 (*a*) I. V. Alabugin, *J. Org. Chem.*, 2000, **65**, 3910–3919; (*b*) I. V. Alabugin and T. A. Zeidan, *J. Am. Chem. Soc.*, 2002, **124**, 3175–3185; (*c*) I. V. Alabugin, G. P. Gomes and M. Abdo, *Comput. Mol. Sci.*, 2018, **9**, e1389; (*d*) Y. Mo, H. Jiao and P. V. R. Schleyer, *J. Org. Chem.*, 2004, **69**, 3493–3499; (*e*) F. Weinhold and C. R. Landis, *Valency and bonding: a natural bond orbital donor-acceptor perspective*, Cambridge University Press, Cambridge, UK, 2005.
14 (*a*) A. S. Perlin and B. Casu, *Tetrahedron Lett.*, 1969, **10**, 2921–2924; (*b*) S. Wolfe, B. M. Pinto, V. Varma and R. Y. N. Leung, *Can. J. Chem.*, 1990, **68**, 1051–1062; (*c*) E. Juaristi and G. Cuevas, *Acc. Chem. Res.*, 2007, **40**, 961–970.
15 X. S. Monfort and O. Eisenstein, *Polyhedron*, 2006, **25**, 339–348.